Journal of Power Sources 194 (2009) 298–302

Contents lists available at ScienceDirect

Journal of Power Sources

journal homepage: www.elsevier.com/locate/jpowsour

Short communication

An unexpected, self-regulating codeposition of nickel and platinum forming deposits with surfaces enriched in platinum

Lise Nicole Menard, Steven H. Bergens*

Department of Chemistry, University of Alberta, Edmonton, Alberta T6G 2G2, Canada

ARTICLE INFO

Article history:
Received 10 March 2009
Received in revised form 24 April 2009
Accepted 27 April 2009
Available online 3 May 2009

Keywords:
Platinum
Nickel
Codeposition
Alkaline
2-Propanol
Direct alcohol fuel cell

ABSTRACT

Galvanostatic depositions onto Ni substrates from 0.2 M $NiCl_2$ in 2.0 M NH_4Cl using a Pt counter electrode are self-regulating, forming rough Pt-Ni deposits with ~1.8 mol% Pt. All or most of the Pt is on the surface of these deposits. Use of added $H_2PtCl_6{\cdot}6H_2O$ as a source of Pt(IV), or $K[PtCl_3(C_2H_4)]{\cdot}H_2O$ as a source of Pt(II), results in Pt-Ni deposits with the Pt dispersed throughout the deposit, with little Pt on the surface. Ni promotes the electrooxidation of 2-propanol over Pt in alkaline electrolytes.

1. Introduction

We report an unexpected electrodeposition of Ni-Pt deposits that contain small amounts of Pt on or near the surface of the deposit. We also report preliminary studies on the electrocatalytic activity of these deposits in alkaline electrolytes. Alkaline fuel cells (AFCs) typically operate between 60 and 90 °C with aqueous potassium hydroxide as the electrolyte [1–3]. Perhaps the most significant advantages of AFCs over acidic fuel cells are that the kinetics of oxygen reduction are faster, and that non-precious metals can be used as electrocatalysts [3]. For example, Ni is active as a hydrogen anode in base [4,5]. Also, Ni increases the activity of Pt and Pt-Ru electrocatalysts towards MeOH oxidation and oxygen reduction [6–21]. Among these reports, the codeposition methods used to prepare Ni-Pt catalysts include borohydride reduction [7,16–18], electrochemical codeposition onto gold [8] and high surface area carbon [13], decomposition of carbonyl complexes [10], and the use of macrocyclic precursors [14,15]. There are also recent reports of Pt depositions onto Ni substrates [22–25] and Ni depositions onto Pt [26–28]. It is believed that Ni enhances the activity of Pt via a bifunctional-type mechanism and/or by altering the electronic properties of Pt in a manner that favors the electrocatalytic reaction.

Direct alcohol alkaline fuel cells (DAAFCs) are investigated as alternatives to their acidic counterparts for the reasons listed above, and because the kinetics of alcohol oxidation are often faster in base [3,29–31]. Further, the migration of ions from the cathode to the anode reduces alcohol crossover in operating DAAFCs [32,33]. The major challenges to the development of DAAFCs are the lack of readily available suitable alkaline membrane electrolytes, and that CO_2 reacts with the electrolyte to form carbonates. We note recent reports of good performance obtained from DAAFCs with polybenzimidiazole membrane electrolytes [34–36]. We recently reported that oxidation of 2-propanol over Pt and Pt-Ru electrocatalysts in alkaline media is facile and does not appear to produce CO_2 at low potentials [37,38]. We now report a codeposition of Ni-Pt from NH_4Cl solutions that self-regulates after small amounts of Pt form on the surface of the deposit. We also report the activities of these deposits towards 2-propanol in base.

2. Experimental

The following reagents were used as received from the supplier: nitrogen (Praxair, prepurified), CO (Praxair, prepurified), NaOH (Alfa Aesar, 99.99%, semiconductor grade), H_2O_2 (EM Science, ACS Grade), $H_2PtCl_6{\cdot}6H_2O$ (Alfa Aesar), $K[PtCl_3(C_2H_4)]{\cdot}H_2O$ (Strem Chemicals), $NiCl_2$ (Aldrich), NH_4Cl (EMD Chemicals), Pt gauze (Alfa Aesar, 25 mm × 25 mm, 52 mesh woven from 0.1 mm diameter wire, 99.9% metal basis), nickel gauze (Alfa Aesar, 100 mesh woven from 0.1 mm diameter wire, 99.9% metal basis), nickel wire (Alfa Aesar, 1 mm diameter wire, 99.9% metal basis), $KMnO_4$ (Fisher Scientific), and Toray carbon paper (untreated, Electrochem EC-TP2-060). The

* Corresponding author. Tel.: +1 780 492 9703; fax: +1 780 492 8231.
E-mail address: steve.bergens@ualberta.ca (S.H. Bergens).

0378-7753/$ – see front matter © 2009 Elsevier B.V. All rights reserved.
doi:10.1016/j.jpowsour.2009.04.073

water was deionized, doubly distilled, and distilled again from alkaline $KMnO_4$ before use. 2-Propanol (Fischer Scientific, suitable for electronic use) was freshly distilled. The Pt counter electrodes were prepared as follows. A Pt gauze was cleaned in 1% H_2O_2, and then blacked in 2 wt% $H_2PtCl_6{\cdot}6H_2O$ in 1 M HCl at 50 mV vs. SHE for 180 min.

Electrochemical experiments were carried out in a typical three-electrode glass cell using a Solartron model SI 1287 Potentiostat controlled with CorrWare version 2.3d software. A constant temperature bath (IKA Labortechnik, RCT basic) equipped with a temperature probe/controller (IKA Labortechnik, ETS-D4 fuzzy) was used to maintain the cell temperature. Inductively Coupled Plasma (ICP-MS) experiments were performed on a PerkinElmer Elan 6000 quadropole ICP-MS equipped with a PerkinElmer AS-91 automated sampler.

Cyclic voltammetry and potentiostatic measurements were carried out by bubbling nitrogen through the electrolyte for 10 min, and then conditioning the working electrode at −0.4 V vs. a reference hydrogen electrode (RHE) for 5 min immediately prior to each experiment. The RHE was made with the same alcohol-free electrolyte. The counter electrode was a blacked Pt gauze behind a 10 μm glass frit. The potential limits, sweep rates, and conditions are outlined in the figure captions and in the text. The potentiostatic electrooxidations were carried out by stepping to the desired potential and holding for 15 min. CO stripping voltammetry was carried out by bubbling CO through the electrolyte with the working electrode at −0.4 V for 30 min, and then cycling the working electrode three times between −0.1 and 1.1 V at 10 mV s^{-1}.

2.1. Galvanostatic deposition of Ni and of Pt-Ni_{Con}

The deposition apparatus consisted of two, 10 cm × 2.5 cm, glass cylinders connected by a 10 μm glass frit. One cylinder contained the Ni gauze working electrode, and the other a 2 cm × 2 cm carbon felt counter electrode. The working and counter electrodes were cleaned in 2% H_2O_2 and rinsed with water before use. The depositions were carried out with stirring at 100 mA for 1 h in 0.2 M $NiCl_2$/2.0 M NH_4Cl (50 mL per glass cylinder). The electrode potentials vs. a standard calomel electrode (SCE) in the working electrode chamber were monitored with a multimeter. The conventional depositions were carried out in the same manner with 250 μL of 0.014 M $H_2PtCl_6{\cdot}6H_2O$ or 0.015 M $K[PtCl_3(C_2H_4)]{\cdot}H_2O$ added to the working electrode chamber.

2.2. Galvanostatic deposition of Pt-$Ni_{PtCounter}$

The deposition was carried out in a 10 cm × 2.5 cm glass cylinder equipped with a stir bar, a Ni gauze working electrode, a blacked Pt gauze counter electrode, and a SCE reference electrode. The working and counter electrodes were cleaned in 2% H_2O_2 and rinsed with water before use. The depositions were carried out with stirring at 100 mA for 1 h in 0.2 M $NiCl_2$/2.0 M NH_4Cl (50 mL). The electrode potentials vs. SCE were monitored with a multimeter. Aliquots were taken at timed intervals for analysis using inductively coupled plasma mass spectrometry.

After the electrochemical experiments, the Pt-$Ni_{PtCounter}$ deposits were dissolved in 30 ml of 1:3 HNO_3:HCl at 100 °C. The solution was then evaporated to dryness, the residue was dissolved in 2% HNO_3, and submitted for ICP-MS analysis to quantify Pt.

3. Results and discussion

We prepared high surface area Ni deposits for this investigation using a modification of the procedure developed by Marozzi et al. [39]. Specifically, rough Ni was galvanostatically deposited onto

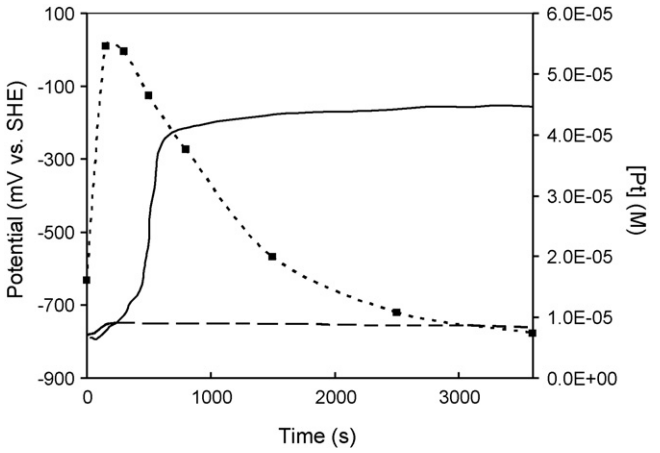

Fig. 1. Working electrode potentials during the galvanostatic deposition of Ni (dashed line) and Pt-$Ni_{PtCounter}$ (solid line) at 0.1 A onto Ni gauzes from 0.2 M $NiCl_2$ in 2.0 M NH_4Cl at 23 °C. The Pt counter electrode potential was ∼1.4 mV during the deposition of Pt-$Ni_{PtCounter}$. Also shown is the [Pt] (squares) during the deposition of Pt-$Ni_{PtCounter}$.

Ni gauze from 0.2 M solutions of $NiCl_2$ in 2.0 M NH_4Cl using a carbon paper counter electrode. The behavior of the deposition was different when Pt was used as the counter electrode. Fig. 1 shows plots of working electrode potential vs. time for the two depositions. All potentials are reported vs. SHE. The working electrode potential stabilized near −760 mV with no observable H_2 evolution with the carbon paper counter electrode. The working electrode potential increased by ∼650 mV over 500 s and then stabilized near −160 mV with significant H_2 evolution with the Pt counter electrode. Fig. 1 also plots the [Pt] vs. time during the deposition with a Pt counter electrode. The [Pt] peaked after 100 s, and then decayed over the remainder of the deposition. The peak in [Pt] occurred when the working electrode potential increased, and when H_2 evolution commenced. The average mass of the deposits made with a Pt counter electrode (Pt-$Ni_{PtCounter}$) was 6.5 mg. The amount of Pt in the deposit (determined by dissolution in acid and ICP-MS) was 0.37 mg, corresponding to 1.8 mol% Pt. In contrast, the typical mass of the pure Ni deposits (made with a carbon paper counter electrode) was 100 mg, a value ∼10 times that of the Pt-$Ni_{PtCounter}$ deposits.

The lower mass of the Pt-$Ni_{PtCounter}$ deposits can be explained by Pt ions from the counter electrode being preferentially deposited onto the working electrode. The presence of Pt on the surface would form a mixed-potential system between the further deposition of metals and H_2 production. Indeed, the standard reduction potentials for Ni^{2+} and Pt^{2+} (−0.257 and 1.180 V) favor the deposition of Pt, and H_2 evolution occurs over Pt but not over Ni under these conditions [40]. Thus, as more Pt is deposited on the surface, an increasing portion of the current would be diverted towards production of H_2, and to this extent, the Pt-$Ni_{PtCounter}$ deposition would be self-regulating.

This explanation would only hold if the majority of the 1.8 mol% of Pt in the Pt-$Ni_{PtCounter}$ is located on, or near the surface of the deposit. A simple yes/no test confirmed that some of the Pt was present at the surface. In dilute H_2O_2, rapid O_2 evolution occurred over a blacked Pt gauze, moderate evolution occurred over Pt-$Ni_{PtCounter}$, and none over pure Ni. Fig. 2 shows the stabilized voltammograms of Pt_{Black}, Ni, and Pt-$Ni_{PtCounter}$ in NaOH electrolyte. The voltammogram of Pt_{Black} is typical of Pt in alkaline electrolytes [41]. The voltammogram of Ni is typical when the upper sweep potential (−380 mV) is below that for formation of β-$Ni(OH)_2$ [42]. The peak corresponds to a $2e^-$ oxidation of Ni to α-$Ni(OH)_2$. The anodic peak was ∼10% larger than the cathodic peak because some

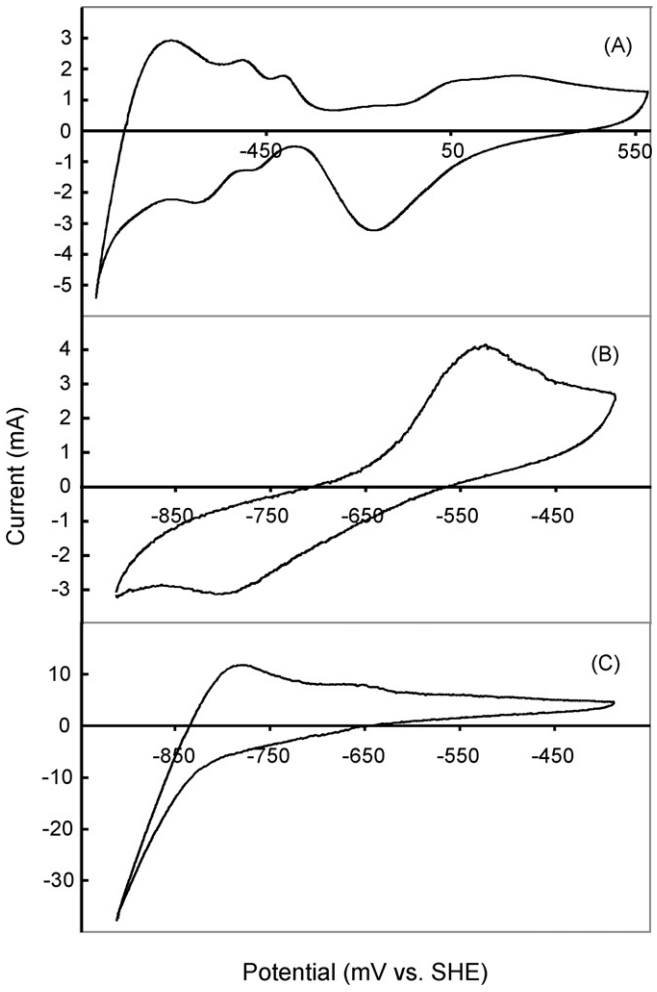

Fig. 2. Cyclic voltammograms of Pt_{black} (A), Ni black (B), and Pt-$Ni_{PtCounter}$ (C) in 0.5 M NaOH, at 10 mV s^{-1} and 23 °C.

hydrogen is formed at the low potential limit [43]. Fig. 2C shows the stabilized voltammogram of the Pt-$Ni_{PtCounter}$ deposit. The hydride region of the anodic sweep as well as the peak for H_2 evolution in the cathodic sweep are characteristic of Pt. Obvious peak characteristics of pure Ni were absent: the most notable is the apparent absence of the α-$Ni(OH)_2$ peak. These observations indicate that the majority of the ~1.8 mol% Pt is located on, or near the surface of the Pt-$Ni_{PtCounter}$ deposit, and that the surface consists of Ni and Pt.

For comparison, we carried out conventional galvanostatic codepositions of Ni and Pt with a carbon paper counter electrode, and with added $H_2PtCl_6{\cdot}6H_2O$ as a source of Pt(IV), or with added $K[PtCl_3(C_2H_4)]{\cdot}H_2O$ as a source of Pt(II) [8,13,44]. The initial [Pt] was similar to the maximum [Pt] during the deposition of Pt-$Ni_{PtCounter}$. Fig. 3 shows that during both depositions, the [Pt] decreased in a manner similar to the deposition of Pt-$Ni_{PtCounter}$. In all other ways, however, the conventional depositions with added Pt ions behaved as the deposition of pure Ni. There was no significant increase in working electrode potential during the first 500 s, and only traces of gas evolution were observed during the deposition. The masses of the conventional Ni-Pt deposits (Pt-Ni_{Con}) were both ~104 mg, ~10 times that of Pt-$Ni_{PtCounter}$. The yes/no H_2O_2 experiment showed no observable O_2 evolution, and the voltammograms of the Pt-Ni_{Con} deposits (Fig. 4) were quite similar to Ni. We note that the anodic α-$Ni(OH)_2$ peak is larger, and there appears to be more hydrogen production at the cathodic limit over Pt-Ni_{Con}, suggesting that more hydrogen is produced at the low potential limit. Regardless,

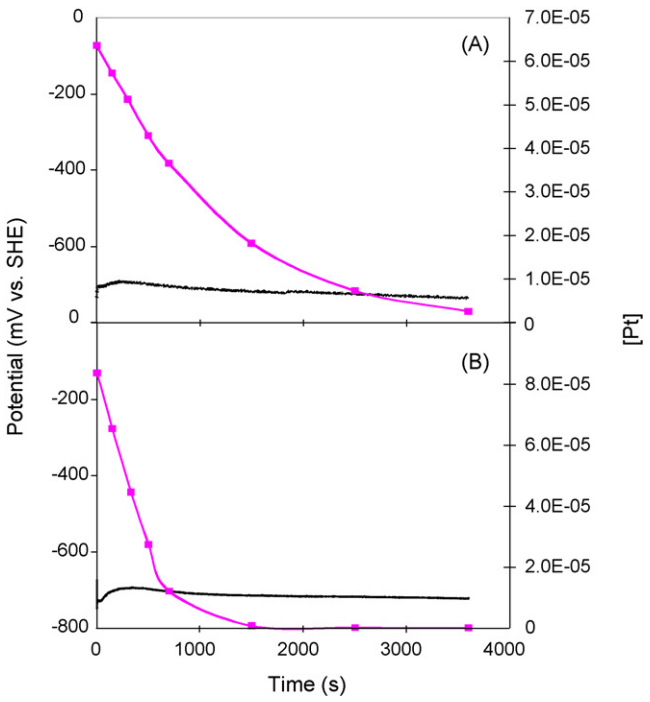

Fig. 3. Working electrode potentials (solid lines) during the conventional galvanostatic codepositions at of Ni and Pt at 0.1 A onto Ni gauzes using $H_2PtCl_6{\cdot}6H_2O$ (A), or $K[PtCl_3(C_2H_4)]{\cdot}H_2O$ (B) as sources of Pt added to 0.2 M $NiCl_2$ in 2.0 M NH_4Cl at 23 °C. Also shown is the [Pt] (squares) during the depositions.

these results show that significantly less Pt is on the surface of Pt-Ni_{Con} than on the surface of Pt-$Ni_{PtCounter}$. ICP-MS experiments did show, however, that ~75% of the added Pt ions were present in both Pt-Ni_{Con} deposits, presumably dispersed throughout the Ni. Thus, the oxidation state of the added Pt alone does not instigate the behavior obtained with a Pt counter electrode. The origins of

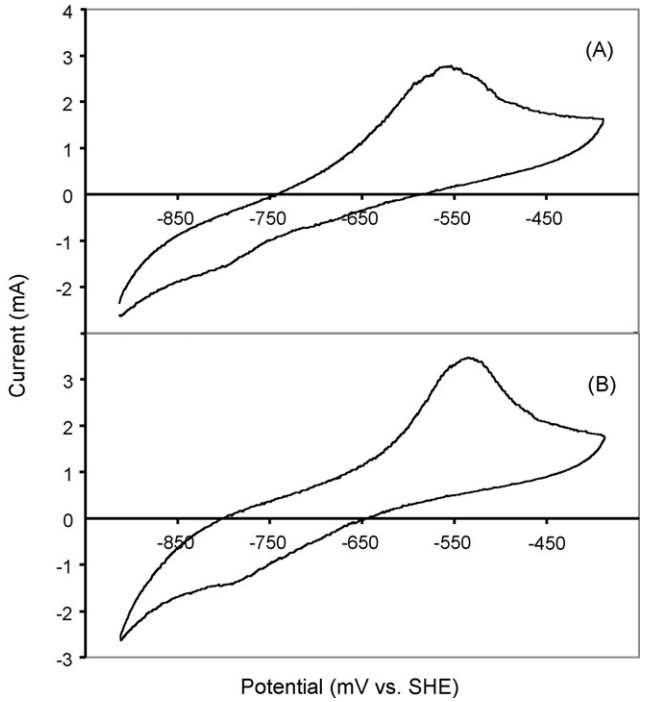

Fig. 4. Cyclic voltammograms of Pt-Ni_{Con} made with $H_2PtCl_6{\cdot}6H_2O$ (A), or $K[PtCl_3(C_2H_4)]{\cdot}H_2O$ (B) in 0.5 M NaOH at 10 mV s^{-1} and 23 °C.

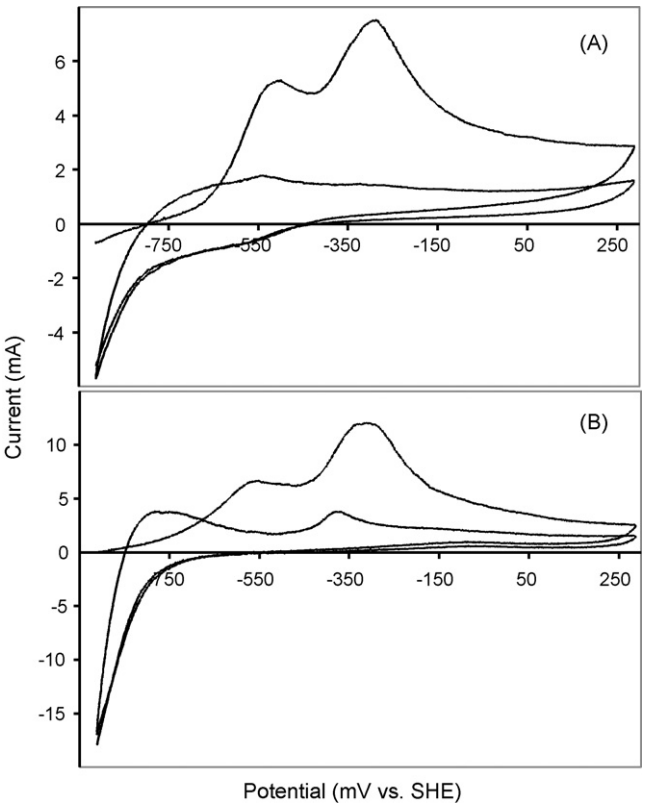

Fig. 5. CO Stripping voltammetry over Ni (A) and Pt-$Ni_{PtCounter}$ (B) in 0.5 M NaOH at 10 mV s^{-1} and 23 °C). CO was adsorbed at −0.4 V for 30 min before the first sweep.

these intriguing differences between the conventional, and the Pt counter electrode depositions are unknown. The most likely explanation is that there are differences between the nature of the Pt ions from the counter electrode and from the added Pt complexes. These differences are responsible for the behavior of the depositions. Further investigations are underway to understand the origins of this phenomenon.

Fig. 5 shows the CO stripping voltammogram of Ni in base [45–48]. The high upper limit that was required to fully oxidize the adsorbed CO also irreversibly oxidized the Ni surface, rendering this procedure a one-time, destructive measurement. The first sweep contained two peaks at −505 and −285 mV. Control experiments without CO showed that the peak at −505 mV resulted from the formation of α-$Ni(OH)_2$, and that the peak at −285 mV resulted from CO stripping. Shervedani et al. observed similar peaks during CO stripping experiments with porous Ni-Zn-P [49]. They proposed that the first peak was primarily due to the oxidation of nickel surfaces in pores that were inaccessible to CO. We found that the total charge under both peaks in the CO-stripping voltammogram was 2.6 times that under the α-$Ni(OH)_2$ peak alone in the baseline voltammogram recorded prior to CO stripping. Thus, similar to Ni-Zn-P, it appears that a portion of the sites on Ni are active towards CO adsorption, while the remainder are active towards formation of α-$Ni(OH)_2$. Based upon these observations, we estimated the electroactive surface area of the Ni deposits by multiplying the α-$Ni(OH)_2$ charge in the baseline voltammogram by 2.6. We regard this method as only a rough estimate of the surface area of Ni until it is confirmed by independent measurements.

Fig. 5 also shows the CO stripping voltammogram of a Pt-$Ni_{PtCounter}$ deposit. The first sweep contains two peaks at −550 and −340 mV that are shifted ∼50 mV in the anodic direction relative to their counterparts over pure Ni. Also in contrast to Ni, a peak at −375 mV remained in subsequent anodic sweeps, and the hydrogen peak in the cathodic sweep was larger. As was the case for Ni, CO stripping over Pt-$Ni_{PtCounter}$ was a one-time, destructive measurement. The total charge under the two peaks in the CO stripping voltammogram was 1.6 times the total anodic charge in the baseline voltammogram recorded prior to the CO stripping experiment. We used this factor to roughly estimate the surface areas of the Pt-$Ni_{PtCounter}$ deposits. A Pt-$Ni_{PtCounter}$ deposit containing 1.8 μmol Pt in total (from ICP-MS) had an estimated surface area ∼3.3 μmol, indicating that the upper limit to amount of Pt at the surface is ∼55 mol%.

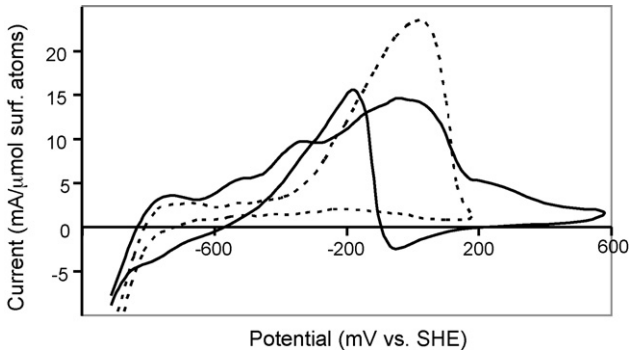

Fig. 6. Potentiodynamic oxidation of 1 M 2-PrOH over Pt-$Ni_{PtCounter}$ (dashed) and Pt_{black} (solid) in 0.5 M NaOH at 10 mV s^{-1} and 60 °C. Currents are normalized to the approximate surface areas of the electrodes.

The high activity of Pt towards 2-PrOH in base is well documented [37,38]. Fig. 6 shows the normalized potentiodynamic oxidations of 2-PrOH over Pt black and Pt-$Ni_{PtCounter}$ in base. Ni was inactive under these conditions. Pt was more active at low potentials, but Pt-$Ni_{PtCounter}$ was more active at high potentials. Thus Ni promotes the activity of Pt towards 2-PrOH at high potentials. The origins of this promoting effect are unknown, but like the well-known promoting effect of Ru on Pt towards MeOH [50], they likely arise from electronic effects and the formation of oxides over Ni [8,9,11,13,16–18,51]. As expected, the Pt-$Ni_{PtCounter}$ deposit was passivated after being swept to high potentials.

Fig. 7 shows the normalized potentiostatic oxidations of 2-PrOH over Pt black and Pt-$Ni_{PtCounter}$. Ni was not appreciably active under these conditions. For each measurement, the electrode was held at −1200 mV for 5 min, then stepped to the desired potential, and the current was recorded over 15 min. The current at 15 min is plotted in Fig. 7. At low potentials, the normalized activity of the Pt-$Ni_{PtCounter}$ was similar to that of Pt_{Black}, except for the absence of the current maximum at −650 mV [37,38]. The activity of the Pt-$Ni_{PtCounter}$ was

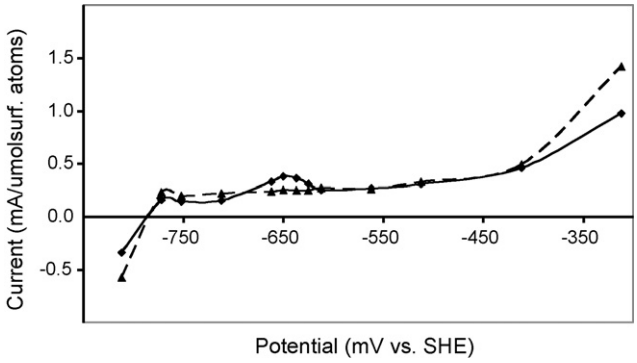

Fig. 7. Normalized currents at 15 min for the potentiostatic oxidation of 1 M 2-PrOH over Pt-$Ni_{PtCounter}$ (dashed triangles) and Pt_{black} (solid diamonds) in 0.5 M NaOH at 60 °C. The estimated surface areas of the Pt-$Ni_{PtCounter}$ and the Pt_{Black} were 3.3 and 9.2 μmol surface atoms, respectively.

significantly higher than Pt_{Black} at −450 mV and above, demonstrating again the promoting effect of Ni at higher potentials.

4. Conclusions

The dependence of the behavior of these depositions on the source of Pt in the electrolyte is unexpected, as is the outcome of the CO stripping experiments suggesting that only a portion of the sites on Ni are active towards CO adsorption. Ni has a promoting effect on the electrooxidation of 2-propanol over Pt that is larger at high potentials. Experiments are underway in these laboratories to further understand the origins of these observations and to determine if this type of deposition has practical applications.

References

[1] G.F. McLean, T. Niet, S. Prince-Richard, N. Djilali, Int. J. Hydrogen Energy 27 (2002) 507–526.
[2] S. Gair, A. Cruden, J. McDonald, T. Hegarty, M. Chesshir, J. Power Sources 154 (2006) 472–478.
[3] J.S. Spendelow, A. Wieckowski, Phys. Chem. Chem. Phys. 9 (2007) 2654–2675.
[4] E. Gülzow, M. Schulze, G. Steinhilber, J. Power Sources 106 (2002) 126–135.
[5] E. Gülzow, Fuel Cells 4 (2004) 251–255.
[6] E. Antolini, J.R.C. Salgado, E.R. Gonzalez, J. Electroanal. Chem. 580 (2005) 145–154.
[7] E. Antolini, Electrochem. Solid State Lett. 8 (2005) A226–A230.
[8] J. Mathiyarasu, A.M. Remona, A. Mani, K.L.N. Phani, V. Yegnaraman, J. Solid State Electrochem. 8 (2004) 968–975.
[9] J.F. Drillet, A. Ee, J. Friedemann, R. Kotz, B. Schnyder, V.M. Schmidt, Electrochim. Acta 47 (2003) 1983–1988.
[10] H. Yang, C. Coutanceau, J.M. Leger, N. Alonso-Vante, C. Lamy, J. Electroanal. Chem. 576 (2005) 305–313.
[11] H.R. Colón-Mercado, H. Kim, B.N. Popov, Electrochem. Commun. 6 (2004) 795–799.
[12] V. Stamenkovic, T.J. Schmidt, P.N. Ross, N.M. Markovic, J. Electroanal. Chem. 554–555 (2003) 191–199.
[13] M.A.A. Rahim, H.B. Hassan, R.M. Abdel Hameed, Fuel Cell 4 (2007) 298–305.
[14] N. Martz, C. Roth, H. Fueb, J. Appl. Electrochem. 35 (2005) 85–90.
[15] M. Goetz, H. Wendt, J. Appl. Electrochem. 31 (2001) 811–817.
[16] K.W. Park, J.H. Choi, S.A. Lee, C. Pak, H. Chang, Y.E. Sung, J. Catal. 224 (2004) 236–242.
[17] J.H. Choi, K.W. Park, B.K. Kwon, Y.E. Sung, J. Electrochem. Soc. 150 (2003) A973–A978.
[18] K.W. Park, J.H. Choi, B.K. Kwon, S.A. Lee, Y.E. Sung, J. Phys. Chem. B 106 (2002) 1869–1877.
[19] T. Toda, H. Igarashi, H. Uchida, M. Watanabe, J. Electrochem. Soc. 146 (1999) 3750–3756.
[20] K.W. Park, J.H. Choi, Y.E. Sung, J. Phys. Chem. B 107 (2003) 5851–5856.
[21] Y. Liang, H. Zhang, Z. Tian, X. Zhu, X. Wang, B. Yi, J. Phys. Chem. B 110 (2006) 7828–7834.
[22] K. Yao, Y.F. Cheng, Int. J. Hydrogen Energy 33 (2008) 6681–6686.
[23] A. Tegou, S. Papadimitriou, S. Armyanov, E. Valova, G. Kokkinidis, S. Sotiropoulos, J. Electroanal. Chem. 623 (2008) 187–196.
[24] S. Papadimitriou, A. Tegou, E. Pavlidou, S. Armyanov, E. Valova, G. Kokkinidis, S. Sotiropoulos, Electrochim. Acta 53 (2008) 6559–6567.
[25] K. Yao, Y.F. Cheng, J. Power Sources 173 (2007) 96–101.
[26] C.-T. Hsieh, J.-Y. Lin, J.-L. Wei, Int. J. Hydrogen Energy 34 (2009) 685–693.
[27] M. Chatenet, Y. Soldo-Olivier, E. Chaînet, R. Faure, Electrochim. Acta 53 (2007) 369–376.
[28] M. Chatenet, R. Faure, Y. Soldo-Olivier, J. Electroanal. Chem. 580 (2005) 275–283.
[29] J.R. Varcoe, R.C.T. Slade, Fuel Cells 5 (2005) 187–200.
[30] N. Fujiwara, S.-I. Yamazaki, Z. Siroma, T. Ioroi, H. Senoh, K. Yasuda, Electrochem. Commun. 11 (2009) 390–392.
[31] E.S. Switzer, T.S. Olson, A.K. Datye, P. Atanassov, M.R. Hibbs, Electrochim. Acta 54 (2009) 989–995.
[32] K. Scott, E. Yu, G. Vlachogiannopolos, M. Shivare, N. Duteanu, J. Power Sources 175 (2008) 452–457.
[33] A.Y. Leykin, O.A. Shkrebko, M.R. Tarasevich, J. Membr. Sci. 328 (2009) 86–89.
[34] A.D. Modestov, M.R. Tarasevich, A.Yu. Leykin, V.Ya. Filimonov, J. Power Sources 188 (2009) 502–506.
[35] H. Hou, G. Sun, R. He, B. Sun, W. Jin, H. Liu, Q. Xin, Int. J. Hydrogen Energy 33 (2008) 7172–7176.
[36] H. Hou, G. Sun, R. He, Z. Wu, B. Sun, J. Power Sources 182 (2008) 95–99.
[37] M.E.P. Markiewicz, D.M. Hebert, S.H. Bergens, J. Power Sources 161 (2006) 761–767.
[38] M.E.P. Markiewicz, S.H. Bergens, J. Power Sources 185 (2008) 222–225.
[39] C.A. Marozzi, A.C. Chialvo, Electrochim. Acta 45 (2000) 2111–2120.
[40] D.R. Lide, CRC Handbook of Chemistry and Physics, 86th ed., CRC Press, Boca Raton, FL, 2005.
[41] J.S. Spendelow, A. Wieckowski, Phys. Chem. Chem. Phys 9 (2007) 2654–2675.
[42] F. Hahn, B. Beden, M.J. Croissant, C. Lamy, Electrochim. Acta 31 (1986) 335–342.
[43] S.A.S. Machado, L.A. Avaca, Electrochim. Acta 39 (1994) 1385–1391.
[44] For another example of an electrochemical Ni/Pt codeposition: R.K. Astakhova, B.S. Krasikov, A.S. Shilina, Rus. J. App. Chem. 59 (1986) 496–500.
[45] K. Wang, G.S. Chottiner, D.A. Scherson, J. Phys. Chem. 96 (1992) 6742–6744.
[46] M. Zhao, K. Wang, D.A. Scherson, J. Phys. Chem. 97 (1993) 4488–4490.
[47] C.F. Zinola, E.J. Vasini, U. Müller, H. Baltruschat, A.J. Arvia, J. Electroanal. Chem. 415 (1996) 165–167.
[48] M. Chatenet, Y. Soldo-Oliver, E. Chaînet, R. Faure, Electrochim. Acta 53 (2007) 369–376.
[49] R.K. Shervedani, A. Lasia, J. Appl. Electrochem. 29 (1999) 979–986.
[50] T. Frelink, W. Visscher, J.A.R. van Veen, Surf. Sci. 335 (1995) 353–360.
[51] S. Mukerjee, S. Srinivasan, J. Electroanal. Chem. 357 (1993) 201–224.